# Drug screens of NGLY1 Deficiency worm and fly models reveal catecholamine, NRF2 and anti-inflammatory pathway activation as clinical approaches

Sangeetha Iyer[1], Joshua D. Mast[1], Hillary Tsang[1], Tamy P. Rodriguez[1], Nina DiPrimio[1], Madeleine Prangley[1], Feba S. Sam[1], Zachary Parton, and Ethan O. Perlstein[1]

[1] Perlara PBC, 6000 Shoreline Court, South San Francisco, California USA

## Abstract

*N*-glycanase 1/*NGLY1* Deficiency is an ultra-rare and complex monogenic glycosylation disorder that affects fewer than 40 patients globally. *NGLY1* Deficiency has been studied in model organisms such as yeast, worms, flies and mice. Proteasomal and mitochondrial homeostasis gene networks are controlled by the evolutionarily conserved transcriptional regulator Nrf1, whose activity requires deglycosylation by NGLY1. Hypersensitivity to the proteasome inhibitor bortezomib is a common phenotype observed in whole animal and cellular models of *NGLY1* Deficiency. Here we describe unbiased phenotypic drug screens to identify FDA approved drugs, generally recognized as safe natural products and novel chemical entities that rescue growth and development of *NGLY1*-deficient worm and fly larvae treated with a toxic dose of bortezomib. We used image-based larval size and number assays for use in screens of a 2,560-member drug repurposing library and a 20,240-member lead discovery library. A total of 91 validated hit compounds from primary invertebrate screens were tested in a human cell line in a NRF2 activity assay. NRF2 is a transcriptional regulator that regulates cellular redox homeostasis and it can compensate for loss of Nrf1. Plant-based polyphenols comprise the largest class of hit compounds and NRF2 inducers. Catecholamines and catecholamine receptor activators comprise the second largest class of hits. Steroidal and non-steroidal anti-inflammatory drugs comprise the third largest class. Only one compound was active in all assays and species: the atypical antipsychotic and dopamine receptor agonist aripiprazole. Worm and fly models of *NGLY1* Deficiency validate therapeutic rationales for activation of NRF2 and anti-inflammatory pathways based on results in mice and human cell models and suggest a novel therapeutic rationale for boosting catecholamine levels and/or signaling in the brain.

**Keywords:** *N*-glycanase 1 Deficiency, *NGLY1*, *SKN-1*, *Pngl*, congenital disorder of deglycosylation, disease model

**Introduction**

NGLY1 Deficiency is the first congenital disorder of deglycosylation (CDDG) described in the biomedical literature (Lam et al., 2017; Enns et al., 2014). NGLY1 Deficiency has multi-organ presentation and clinical features in patients such as global developmental delay, a complex hyperkinetic movement disorder, small body size, seizures, and alacrimia. *NGLY1* is an ancient gene encoding a cytosolic enzyme called *N*-glycanase 1 – also referred to as PNGase – which catalyzes the hydrolysis and release of *N*-glycans from *N*-glycosylated proteins (Suzuki et al., 2016). NGLY1 is thought to function primarily in an evolutionarily conserved protein surveillance and disposal pathway called ERAD, or endoplasmic reticulum-associated degradation (Suzuki et al., 2015). NGLY1 also regulates the activity of specific glycoproteins by using deglycosylation as a post-translational on/off switch. Cellular models of NGLY1 Deficiency have shown that the transcriptional regulator Nrf1 is a specific deglycosylation target of NGLY1 and that knocking out *NGLY1* phenocopies knocking out *Nrf1* (Tomlin el al., 2017). Only deglycosylated Nrf1 can be proteolytically processed into the mature nuclear-active form. Once in the nucleus, Nrf1 controls the expression of proteasomal subunit genes in response to protein folding stress in mammalian cells (Radhakrishnan et al., 2014), worms (Lehrbach & Ruvkun, 2016) and flies (Grimberg et al., 2011). In flies NGLY1 regulates the glycosylation status of the ortholog of a bone morphogenetic protein (BMP) signaling ligand (Galeone et al., 2017). Demonstrating the complexity of how loss-of-function mutations in the gene lead to pathophysiology in humans, NGLY1 regulates mitochondrial physiology in human and mouse fibroblasts and in worms through mechanisms that are still under investigation (Kong et al. 2018). Interestingly, mitophagy defects caused by loss of Nrf1 function can be rescued by activation of the related transcriptional regulator NRF2, which controls the expression of genes involved in antioxidant and redox stress responses (Yang et al., 2018).

In the five years since the publication of the first *NGLY1* Deficiency diagnostic cohort of eight patients (Enns et al., 2014) multiple research groups have contributed to our understanding of disease-causing and loss-of-function mutations in the *NGLY1* gene and its orthologs by generating and characterizing small and large animal models as well as patient-derived cell models. From this marketplace of disease models, a common phenotype emerged: hypersensitivity to proteasome inhibition by bortezomib (Fenteany et al., 1995). In worms, hypersensitivity to bortezomib toxicity was observed in an otherwise normally developing *PNG-1*/*NGLY1* null mutant, which has a half-maximal growth inhibitory concentration ($IC_{50}$) several

2

hundred times lower than wildtype worms (Lehrbach & Ruvkun, 2016). Using a chemically related proteasome inhibitor lacking the reactive boronic acid group, it was shown that mouse embryonic fibroblasts derived from *NGLY1*-knockout mice and *NGLY1*-knockdown human cell lines are several-fold more sensitive to carfilzomib toxicity compared to controls (Tomlin et al., 2017).

In an effort to phenotype and screen a homozygous loss-of-function *Pngl*/*NGLY1* fly modeling the patient-derived C-terminal premature stop codon allele R401X, we showed that $Pngl^{-/-}$ homozygous mutant larvae are 25-fold more sensitive than heterozygotes to the toxic effects of bortezomib (Rodriguez et al., 2018). Another group reported that a *Pngl* RNAi-knockdown fly model of *NGLY1* Deficiency has constitutively reduced expression of Nrf1-dependent proteasomal subunit genes, consistent with findings of hypersensitivity to bortezomib toxicity in the other models (Owings et al., 2018). Loss of NGLY1 causes intolerance to bortezomib that is as evolutionarily conserved as the underlying Nrf1-dependent proteasome bounce-back response because they go hand in hand. The prediction that has been confirmed so far only in mammalian cells is that NGLY1 and its orthologs Pngl in flies and PNG-1 in worms deglycosylate Nrf1 and its homologs cap 'n' collar in flies and SKN-1 in worms. We reason that small molecule suppressors of bortezomib will safely activate bypass pathways that rescue or compensate for loss of NGLY1 in a whole animal and will have a higher probability of exhibiting a favorable therapeutic index in mammals.

We used our $Pngl^{-/-}$ fly model in a drug repurposing screen to identify compounds that rescue larval developmental delay (Rodriguez et al., 2018). Homozygote flies fail to thrive in the absence of any exogenous stressor or enhancer such as bortezomib. There are two limitations of our previous screen. First, flies homozygous for a patient-derived nonsense allele are extremely sick and only one fly-specific validated hit was identified – the insect molting hormone 20-hydroxyecdysone. Second, flies homozygous for a patient-derived nonsense allele are further sickened by the organic solvent dimethyl sulfoxide (DMSO) in which all test compounds are solubilized, and all stock solutions prepared. Therefore, drug screens were conducted at the limit of detection and a high false negative rate was due to under-dosing of test compounds.

Here we addressed the shortcomings of the initial fly-only drug repurposing campaign. First, we discovered that the $Pngl^{+/-}$ heterozygote is two-fold more sensitive to bortezomib toxicity than

wildtype animals, it tolerates DMSO, and it has no detectable developmental delay. We hypothesize that it will be easier for a small molecule to suppress larval developmental delay in bortezomib-treated healthy heterozygotes versus constitutively sick homozygotes because otherwise healthy heterozygotes tolerate higher levels DMSO and thus allow for all test compounds to be screened at a five-fold higher concentration. Second, we extended the bortezomib intolerance results of Lehrbach & Ruvkun to a liquid-based, 384-well-plate quantitative worm larval growth and development assay for drug screening. We hypothesize that a two-species bortezomib-suppressor screen conducted in parallel would reveal hit compounds that target evolutionarily conserved disease modifiers and disease-modifying pathways. Third, we not only cross-tested all hit compounds from the primary worm screen in the fly assay, and vice versa, but we also cross-tested all hit compounds in two different worm assay paradigms (bortezomib treatment versus carfilzomib treatment), in two different fly assay paradigms (bortezomib treatment of heterozygotes versus homozygotes), and in a human cell NRF2 transcriptional activity reporter assay. This cross-validation scheme generated a short list of generic drugs and nutriceuticals in which we had the highest degree of confidence of reproducibility and clinical trial actionability. Finally, we screened not only the same repurposing library as described in Rodriguez *et al* but also a ten-fold larger lead discovery library. We hypothesize that in some instances the same known mechanisms of action of repurposable drugs will be targeted by novel chemical entities, which serve as starting points for lead optimization toward a best-in-class clinical candidate.

**Materials and Methods**

*Strains and compound libraries*
The *png-1* deletion mutant ok1654 was previously described (Lehrback & Ruvkun, 2016) and is available from the CGC Stock Center (strain ID: RB1452). The nonsense allele *Pngl* fly was previously described (Rodriguez et al., 2018) and is available from the Bloomington Stock Center. The 2,560-compound Microsource Spectrum Collection was available for purchase before the distributor went out of business. The 20,240-compound lead discovery library was purchased from Chembridge Corporation. All compounds were dissolved in DMSO and stored at -80˚C in Labcyte-compatible LDV plates until use.

*High-throughput larval growth assays in worms*

Positive controls for all screens are *png-1* mutants + DMSO (vehicle control) and the negative controls are *png-1* mutants + DMSO + 205nM bortezomib. Both drug libraries were screened in triplicate with controls on each 384-well drug screening plate. Using the Echo550 (Labcyte Inc.), Bortezomib was acoustically dispensed into the destination plates the day before the worm larvae sort. 5µL of HB101 bacteria were dispensed into 384-well plates, containing S Medium in each well. Using the BioSorter (Union Biometrica), 15 L1 *png-1* mutant larvae were sorted into each well, and plates were incubated at 20˚C while shaking. After five days of incubation, 15µL of 8mM sodium azide was added to each well to immobilize worms prior to imaging in a custom worm imager. Finally, automated image processing was run on each plate.

*High-throughput fly larval growth assays*

Drug screens of *Pngl* heterozygous flies were conducted in the presence of 9µM bortezomib. The negative controls in the screen are *Pngl* heterozygous flies + DMSO + bortezomib and the positive controls are *Pngl* heterozygous flies + DMSO. Both drug libraries were screened in triplicate. Using the Echo550 (Labcyte Inc.), test compound was acoustically dispensed and standard fly food media (molasses, agar, yeast, propionic acid) lacking cornmeal, but carrying 0.025% bromophenol blue was dispensed using a Multi-Flo (Bio-Tek Instruments) into each well of a 96-well plate. Then, the BioSorter was used to dispense *Pngl* heterozygous larvae, three per well. At three days post incubation with the compounds, the plates were scored for larval size rescue in a custom fly imager.

*High-throughput drug screening and analysis*

Hit compounds rescued worm development, i.e., increased the number of worms (total area taken up by worms) in the well. Therefore, the output of the image processing was worm area per well. Quality control was performed to ensure that the control well grew as expected, the *png-1* mutants are sensitive to bortezomib as expected, there are no obvious plate effects, and dispense errors were eliminated. We also manually verified each well by visual analysis after the unbiased quantitative analysis to make sure no false positives were counted as true hits. We count wells as hits that have a Z-score greater than 2 across all three replicates of the screen and were free of image artifacts.

Fly screening conditions were previously described (Rodriguez et al., 2018). Briefly, we imaged the plates using a custom fly imager and analysis tool to determine the area the larvae occupy per well. Then, we counted the number of larvae per well to normalize the total area per well data and identified suppressors of the phenotype. We also manually scored the wells for contaminants that may give false positives.

*Keap1-NRF2 activation luciferase reporter assay in O2OS cells*

We tested compounds using the PathHunter® eXpress Keap1-NRF2 Nuclear Translocation Assay (DiscoverX, San Diego). Briefly, PathHunter cells are plated and incubated for 24 hours at 37°C. 10µL of test compound was added and cells were incubated with compound for 6 hours at room temperature. Working detection reagent solution was added and plates were incubated for 60 minutes at room temperature. Chemiluminescence signal was read by a SpectraMax M3.

**Results**

**Developing high-throughput bortezomib-modifier assays for nematode and fly larvae**

The nematode ortholog of *NGLY1* is *PNG-1*. The strain used here is ok1654, which contains an 800-base-pair deletion in the *PNG-1* open reading frame resulting in a null mutant. We confirmed that ok1654 does not have an intrinsic growth defect but is markedly hypersensitive to bortezomib toxicity (**Figure 1A**). Bortezomib exacerbates the proteasomal stress that NGLY1-deficient worms are already experiencing because of the concomitant loss of Nrf1 activity and results in an exaggerated disease phenotype, in this case early larval growth arrest (Lehrbach & Ruvkun, 2016). From the bortezomib dose-response curve we established that a *png-1* null mutant is sensitive to bortezomib toxicity down to the low nanomolar range. After further optimization studies, we selected 205nM bortezomib as the concentration for the primary screens and for secondary retest and cross-test experiments to validate hit compounds.

The ortholog of *NGLY1* in flies is *Pngl*. We previously developed a *Pngl*^{-/-} fly model based on a recurrent C-terminal nonsense allele found in NGLY1 patients, optimized a high-throughput larval size assay, and screened a 2,560-member drug repurposing library on *Pngl*^{-/-} larvae (Rodriguez *et al*, 2018). That effort culminated in a single validated hit compound, 20-hydroxyecdysone (20E). 20E is an insect-specific sterol-derived molting hormone. In order to identify clinically actionable hits, we increased the overall hit rate and robustness of fly screens.

We established a bortezomib toxicity dose-response curve for $Pngl^{+/-}$ heterozygote larvae and determined that these animals are two-fold more sensitive than wildtype animals (**Figure 1B**). After further optimization studies, we selected 9µM bortezomib as the concentration for the primary screens and for secondary retests and cross-tests to validate hit compounds.

**Worm repurposing screen and hit validation**

In the presence of 205nM bortezomib, *png-1* null mutant worms arrest as L1 larvae while wildtype animals treated with the same dose of bortezomib develop normally. A worm repurposing hit is defined as a compound that rescued bortezomib-treated *png-1* null worms such that their size and number were indistinguishable from control wells containing vehicle-treated *png-1* null worms. All test compounds were screened at a final concentration of 25µM. Images of a representative positive control well and a representative negative control well, and two examples of wells containing suppressors and enhancers/toxic compounds are shown in **Figure 2A**. The Venn diagram in **Figure 2B** summarizes the overlap of screening positives between three independent replicates. A total of 63 suppressors have Z-scores greater than two in all three replicates. The hit rate for worm suppressors is 63/2560 or 2.5%. A total of 51 enhancers have Z-scores less than two in all three replicates. The hit rate for enhancers/toxic compounds is 51/2560 or 2%. Enhancers/toxic compounds were not further investigated in this study. 60/63 worm suppressors were available for reorder as fresh powder stocks, retested in the primary bortezomib assay paradigm, and then scored in a secondary non-bortezomib assay paradigm.

Some compounds can directly inactivate bortezomib which leads to a false positive result. For example, polyphenols and in particular polyphenols containing multiple catechols are known to form covalent adducts with bortezomib by boronate-catechol complexation (Glynn et al., 2015; Golden et al., 2009). In order to filter out those compounds, we tested the 60 worm suppressors on the *png-1* null mutant treated with the chemically related proteasome inhibitor carfilzomib, which lacks the reactive boronic acid that renders bortezomib vulnerable to covalent attack. We established a carfilzomib dose-response curve for *png-1* null mutant worms (**Supplemental Figure 1**). We directly compared these data to worms treated with 205nM bortezomib in order to determine at which concentration we observe comparable larval growth arrest. We retested all 60 worm suppressors in the presence of 27.3µM carfilzomib, meaning carfilzomib is significantly less potent than bortezomib.

A total of 48/60 (80%) worm suppressors retested in the bortezomib assay paradigm. 15/60 (25%) worm suppressors scored positively in the carfilzomib assay paradigm. Overall, 15/60 (25%) worm suppressors rescued in both worm assay paradigms, i.e., in the presence of either bortezomib or carfilzomib. Those 15 compounds are the worm repurposing hits: aripiprazole, benserazide, ellagic acid, epicatechin monogallate, epigallocatechin-3-monogallate, ethylnorepinephrine, gossypetin, koparin, phenylbutazone, pomiferin, purpurogallin-4-carboxylic acid, quercetin, theaflavin monogallate, triamcinolone, and 3,4-didesmethyl-5-deshydroxy-3'-ethoxyscleroin.

10/15 (66%) worm repurposing hits are plant-based polyphenols. Epicatechin monogallate and epigallocatechin-3-monogallate are structural analogs, the latter containing an additional hydroxyl group. They are both abundant in tea leaves. The two plant flavonols quercetin and gossypetin are structural analogs, the latter containing an additional hydroxyl group. Quercetin is found in many foods and gossypetin is found is *Hibiscus* flowers. Aripiprazole, benserazide and ethylnorepinephrine act on catecholamine levels and/or signaling in the brain. Phenylbutazone is a decades-old first-generation non-steroidal anti-inflammatory drug, or NSAID, but is not currently approved and marketed in the United States. Triamcinolone is a synthetic corticosteroid and generic topical anti-inflammatory drug.

**Fly repurposing screen and hit validation**

In the presence of 9μM bortezomib, *Pngl*$^{+/-}$ flies are developmentally delayed as first-instar larvae. A fly repurposing hit is defined as any compound that in triplicate rescued bortezomib-treated *Pngl*$^{+/-}$ larval growth and size such that they were indistinguishable from control wells containing DMSO-treated heterozygotes. All test compounds were screened at a final concentration of 32μM. Separation between positive and negative control wells is shown in **Figure 2C**. As expected, most test compound wells do not affect bortezomib-treated heterozygotes as determined by quantifying larval area per well and remain close to the negative control Z-score, (**Figure 2D**). We identified 31 fly suppressors that rescued larval size with Z-score greater than 2.5 in at least two out of three replicates, yielding a hit rate of 1.2%, or half the hit rate of the worm repurposing screen (**Supplemental Figure 2**) but thirty times the hit rate of the previously published *Pngl*$^{-/-}$ drug repurposing screen (Rodriguez et al., 2018).

In order to eliminate suppressors that directly inactivate bortezomib or that fail to rescue in the absence of bortezomib-induced proteasomal stress, we retested suppressors in a 12-well petri dish assay at 0, 10μM, 50μM, 100μM of compound on either $Pngl^{+/-}$ larvae in the presence of bortezomib or $Pngl^{-/-}$ larvae without bortezomib. We could not retest suppressors in a carfilzomib assay paradigm because $Pngl^{+/-}$ larvae were resistant to carfilzomib toxicity at the highest concentration tested. Note in the DMSO-hypersensitive homozygous animals that we might not observe rescue at 100μM because of the increased amount of DMSO (0.2%) needed to test that concentration of compound. Although we did not confirm by chemical analysis, any compound that strongly rescued only in the bortezomib assay paradigm is likely a bortezomib inactivator. The top candidate bortezomib inactivators are tannic acid and gossypetin (**Supplemental Material**). Gossypetin contains two catechols per molecule and tannic acid contains five catechols per molecule. These two compounds are the only overlapping primary screening hits between the worm and fly repurposing screens.

30/31 fly suppressors were reordered as fresh powder stocks (one compound failed to dissolve at 10mM as stock solution). 21/30 (70%) fly suppressors retested in the primary heterozygote assay paradigm, which is comparable to the retest rate of worm suppressors. 20/30 (66%) fly suppressors scored positively in the secondary homozygote assay paradigm. 13/30 (43%) suppressors validated in both homozygote and heterozygote assay paradigms, which is higher than the worm cross-validation rate. Those 13 compounds are the fly repurposing hits: aminacrine, aripiprazole, β-Amyrin, butopyronoxyl, clindamycin, dyphylline, L-glutamine, ketorolac tromethamine, lumefantrine, promazine, pyrimethamine, quinizarin and thioguanosine.

In contrast to the worm repurposing hits which fell into two pharmacological classes, the fly repurposing hits span a range of mechanisms, only one of which appears to be fly-specific, e.g., the insect repellent butopyronoxyl. Ketorolac is a first-generation NSAID class but is structurally distinct from the worm repurposing hit and NSAID phenylbutazone. β-Amyrin is triterpene natural product with anti-inflammatory effects. Aside from aripiprazole, the remaining fly repurposing hits appear to be mechanistic singletons and do not have obvious functional or structural analogs with worm repurposing hits. There are two antimalarial compounds, pyrimethamine and lumefantrine, and two DNA-damaging cancer drugs, aminacrine and thioguanosine. Dyphylline is a xanthine derivative with bronchodilator and vasodilator effects. Clindamycin is a lincosamide antibiotic used for a range of bacterial infections.

**Cross-validation of worm and fly repurposing hits**

In order to quantify the overlap between worm and fly repurposing hits, we selected 11 worm repurposing hits for cross-testing in both fly assay paradigms, and 19 fly repurposing hits for cross-testing in both worm assay paradigms. The fraction of worm repurposing hits that rescue in flies is higher than the fraction of fly repurposing hits that rescue in worms. 11/11 (100%) of worm repurposing hits scored positively in the fly heterozygote assay paradigm. 6/11 (55%) of these compounds cross-validated in both fly assay paradigms.

However, 3/19 (16%) fly repurposing hits scored positively in the worm bortezomib paradigm. 3/19 (16%) fly repurposing hits scored positively in the worm carfilzomib paradigm. Only 1/19 (5%) fly repurposing hit cross-validated in both worm assay paradigms: aripiprazole. Of the 30 repurposing hits that were cross-tested, seven compounds (23%) are active both worm assay paradigms and in both fly assay paradigms: aripiprazole, benserazide, phenylbutazone, pomiferin, quercetin, theaflavin monogallate and 3,4-didesmethyl-5-deshydroxy-3'-ethoxyscleroin. Their chemical structures are shown in **Figure 3**.

Aripiprazole is an atypical antipsychotic drug approved for use alone or in combination in adults and children for the treatment of symptoms of many CNS diseases, including schizophrenia, autism spectrum disorder and bipolar disorder (Shapiro et al., 2003; Kikuchi et al., 1995). Aripiprazole has been available in generic form since 2015. Benserazide is an aromatic L-amino acid decarboxylase inhibitor which has been co-administered with levodopa (L-Dopa) for decades to boost dopamine levels in the brain in the treatment of Parkinson disease. As mentioned above, phenylbutazone is decades-old NSAID and quercetin is plant flavonol with complex pharmacology, including anti-inflammatory effects. Theaflavin monogallate is a polyphenol found in black tea leaves. Pomiferin is prenylated isoflavone found in osage orange trees.

**Drug discovery screens, secondary retests and cross-validation of novel hit compounds**

Using the same screening conditions and hit-calling analysis as the worm repurposing screen, we scaled up efforts with *png-1* null mutant larvae and a 20,240-member lead discovery library. We identified 28 novel worm suppressors and 6 novel worm enhancers/toxic compounds with a combined hit rate of 0.143% (**Figure 4A; Supplemental Material**). Enhancers/toxic compounds were not further investigated in this study. 12/28 (43%) novel worm suppressors retested in the

bortezomib assay paradigm. 10/28 (36%) novel worm suppressors scored positively in the carfilzomib assay paradigm. A total of five novel worm suppressors (18%) validated in both paradigms, which is comparable to the cross-validation rate observed for worm repurposing hits. Consistent with the results of the repurposing screens, the fraction of novel worm suppressors that are active in flies is higher than the fraction of novel fly suppressors that are active in worms. 4/5 (80%) of novel worm suppressors cross-validated in both fly assay paradigms.

Using the same screening conditions and hit calling analysis for the fly repurposing screen, we scaled up efforts with $Pngl^{+/-}$ larvae and a 20,240-member lead discovery library. We identified 16 novel fly suppressors, resulting in hit rate of 0.07% (**Figure 4B; Supplemental Material**). 15/16 novel fly suppressors were reordered as fresh powder stocks. 10/15 (67%) novel fly suppressors retested in the primary heterozygote assay paradigm. 13/15 (87%) novel fly suppressors scored positively in the secondary homozygote assay paradigm. A total of 10 novel fly suppressors (67%) validated in both paradigms. Of the 13 novel fly suppressors, 12 were retested in both worm assay paradigms. None of the novel fly suppressors scored positively in the bortezomib assay paradigm, but 8/12 (66%) compounds scored positively in the worm carfilzomib assay paradigm.

The known NRF2 activator sulforaphane did not rescue in either worm assays but it did score positively in the $Pngl^{-/-}$ homozygote assay paradigm, rescuing this mutant to 50% of the control (**Supplemental Material**). In the most striking example of overlap between the repurposing library and discovery library, we identified two novel fly suppressors that are structural analogs of pyrimethamine, sharing a diaminopteridine group present in folic acid analog inhibitors of DNA synthesis enzymes, such as methotrexate. Both pyrimethamine and the two novel fly suppressors rescue homozygotes to near 100% of the heterozygote control. A second novel fly suppressor also rescues homozygotes to near 100% of the heterozygote control.

**Keap1-NRF2 activation assay in human cells**

A total of 91 repurposing hits and novel suppressors from both worm and fly screens were cross-tested in a Keap1-NRF2 activation assay in the U2OS osteosarcoma cell line. 7/91 (8%) compounds are active up to a 30μM half-maximal effective concentration ($EC_{50}$) cutoff (**Table 1**). Listed here in order of percentage of maximal response normalized to the positive control CDDO methyl ester: aripiprazole (78%) = pyrogallin (78%) > fisetin (59%) > purpurogallin-4-

carboxylic acid (53%) = 3-methoxycatechol (50%) > rhamnetin (43%) > pyrimethamine (27%). Of these seven only fisetin has been previously shown to activate NRF2 target gene expression (Smirnova et al., 2011). To increase confidence in the assay, we also tested three additional known NRF2 inducers: sulforaphane, omaveloxolone and dimethyl fumarate. None of the novel lead worm or fly suppressors are NRF2 inducers.

## Discussion

In summary, we demonstrated the therapeutic relevance of unbiased phenotypic drug screens of worm and fly models of NGLY1 Deficiency. We addressed the major shortcoming of our previous drug screening effort by increasing hit rate and reproducibility with the more permissive $Pngl^{+/-}$ heterozygote assay as the primary screen followed by a secondary retest in the more restrictive $Pngl^{-/-}$ homozygote assay paradigm, which selected for the subset of hit compounds that specifically rescues loss of NGLY1. We addressed the other significant shortcoming of our previous drug screening effort by including worms as a second species in the primary screening stage, which increased the total number and mechanistic diversity of hits. And by including human cells as a third species in the hit validation stage we selected for hit compounds that act on conserved targets and pathways. We identified three clinic-ready therapeutic approaches by focusing on the subset of hit compounds that rescue larval growth and development in both worms and flies and in the presence and absence of bortezomib: (1) NRF2 activators/inducers; (2) catecholamine boosting drugs; (3) anti-inflammatory drugs. Only one compound was found to be active in all three species (worm, fly and human cells) and in all assay paradigms (plus bortezomib, plus carfilzomib, and NRF2 reporter): aripiprazole.

Before discussing why we observed those three pharmacological classes and the evidence that supports their testing in clinical trials, we consider reasons why any given hit compound might be active in one or a combination of the species and assay paradigms tested herein. Some reasons have to do with compound stability, compound solubility, bioavailability, drug metabolism and pharmacokinetics, not to mention the differences between worm screens versus fly screens. The following is by no means an exhaustive list of salient factors. Worm screens were all performed in simple liquid media that is a buffered salt solution plus essential nutrients and contains bacteria as a food source. By contrast, the fly screens were performed in a nutrient-rich solid media ("fly food") with a molasses base. The worm screen is a six-day assay that spans all stages

of the worm life cycle while the fly screen is a three-day assay that only spans the larval stages of fly development. The worm screen was performed with 205nM bortezomib while the fly screen was performed with 9µM bortezomib.

Other reasons why a hit compound is active in one species but not the other may have to do with pharmacodynamics, that is the drug targets are not evolutionarily conserved or the drug binding sites of shared drug targets are too divergent between worm and fly orthologs. Resolving which pharmacokinetic and pharmacodynamic variables and their relative contributions explain the failure of a hit compound in any given assay or species paradigm is a very important research question that is beyond the scope of the present study. However, what we can conclude from this study is that NRF2, anti-inflammatory and catecholamine pathways are evolutionarily conserved between worms, flies and human cells.

Indeed, NRF2 pathway activators and anti-inflammatory drugs have been proposed as clinical approaches to address the underlying defects in mitochondrial physiology observed in *NGLY1*-deficient cells, specifically a defect in mitophagy and excessive mitochondrial fragmentation (Yang et al., 2018). In addition to its more well studied role as a transcriptional regulator of the proteasome bounce-back response, Nrf1 also controls the expression of mitochondrial homeostasis and mitophagy gene not only in human cells but also in worms (Paek et al., 2012) and flies (Tsakiri et al., 2013). A unifying theory of NGLY1 Deficiency is that disease phenotypes are primary or secondary consequences of the loss of conserved Nrf1-dependent gene expression programs in cell types and tissues that are vulnerable to proteotoxic, oxidative or redox stress. A recent n=1 clinical study of a NGLY1 patient who died of complications due to adrenal insufficiency suggest that steroidogenic secretory tissues fit the criteria of a vulnerable cell type (van Keulen et al., 2019). The *Pngl*$^{-/-}$ fly has defects in its physiologically analogous neuroendocrine tissues that fail to produce and secrete the cholesterol-derived hormone 20-hydroxyecdysone (Rodriguez et al., 2018).

Why do anti-inflammatory drugs rescue worm and fly models of NGLY1 Deficiency? Defects in mitophagy lead to release of mitochondrial genomic DNA and mitochondrial-encoded RNA from fragmented and damaged mitochondria into the cytoplasm drives constitutive STING and related innate immunity responses in *NGLY1*$^{-/-}$ mice and cell lines (Yang et al., 2018). These innate immunity pathways are conserved in flies (Martin et al., 2018) and worms (Wu et al.,

13

2014). We predict that mitochondrial fragmentation and mitophagy defects are present in cells and tissues of *png-1* null mutant worms and *Pngl*^{-/-} flies. Mitophagy defects and oxidative stress were in observed in *SKN-1* mutant worms (Palikaras et al., 2015). We hypothesize that the steroidal and nonsteroidal anti-inflammatory drugs that rescue worm and fly models of *NGLY1* Deficiency, e.g., phenylbutazone, are suppressing basally elevated innate immune responses. It's tempting to speculate that hyperactive innate immunity responses contribute to larval growth arrest and developmental delay in NGLY1-deficient animals and that these anti-inflammatory responses are dampened by inhibitors of DNA synthesis, specifically purine biosynthetic enzymes targeted by the fly repurposing hits thioguanosine and the dihydrofolate reductase-like inhibitor pyrimethamine (Dziekan et al., 2019), and possibly the diaminopteridine-containing novel lead compounds that resemble pyrimethamine. Even more so because the same mechanism of action appears to have been revealed by parallel repurposing and discovery screens.

At this time, catecholamine boosters are supported by measurements of reduced catecholamine precursors in the cerebral spinal fluid of NGLY1 patients (Lam et al., 2017), as well as the fact that an adult and wheelchair-bound NGLY1 patient has received the dopamine precursor levodopa. Future natural history studies of *NGLY1* Deficiency should focus on catecholamine insufficiency as a potential driver or axis of pathophysiology. The effects of aripiprazole in worms depends on catecholamine pathway genes (Osuna-Lugue et al., 2018). In flies, aripiprazole was shown to reduce the levels of an aggregated polyglutamine-expanded mutant protein in a model of Machado-Joseph disease, or spinocerebellar ataxia type 3 (Costa et al., 2016). The mechanism of rescue appears to rely on activation of proteotoxic and antioxidant stress responses. It is tempting to conjecture that aripiprazole achieved its rescue effects in the Machado-Joseph fly model and in our *NGLY1* Deficiency fly model by activating both NRF2 and catecholamine pathways; and further that the unique polypharmacology of aripiprazole combines catecholamine pathway activation and NRF2 pathway activation.

## Acknowledgements

**Table 1**. Keap1-NRF2 transcriptional activity reporter data

| Compound Name | EC50 (µM) | Hill | Max Response |
|---|---|---|---|
| CDDO methyl esther | 0.01389697 | 1.556 | 100.31 |
| Sulforaphane | 0.297622 | 1.5274 | 106.9 |
| Omaveloxolone (RTA 408) | 0.2115237 | 3.6273 | 90.953 |
| PYROGALLIN | 2.471992 | 1.0653 | 77.874 |
| FISETIN | 2.503583 | 1.6383 | 58.956 |
| RHAMNETIN | 2.380603 | 1.0183 | 43.274 |
| Dimethyl fumarate | 4.78086 | 1.5699 | 119.38 |
| PURPUROGALLIN-4-CARBOXYLIC ACID | 5.528483 | 1.7406 | 53.14 |
| 3-METHOXYCATECHOL | 15.76957 | 1.6907 | 50.248 |
| ARIPIPRAZOLE | 30.33891 | 5.0303 | 78.294 |
| PYRIMETHAMINE | 29.82909 | 3.7568 | 27.003 |

**Figure Legends**

**Figure 1**. Bortezomib dose-response experiments of *png-1* homozygous mutant worms (**A**) and *Pngl* heterozygous mutant flies (**B**).

**Figure 2**. 2,560-compound drug repurposing screens of *png-1* homozygous mutant worms and *Pngl* heterozygous mutant flies. (**A**) Worm screen images of a representative positive control well (A01), a representative negative control well (C23), two presumptive suppressors (K12, K13), and two presumptive enhancers/toxic compounds (C18, N14). (**B**) Venn diagram of overlapping hits from three replicate screens. (**C**) Z-score plot of three replicates of fly repurposing screen positive control (red circles) versus negative control (cyan circles) wells. (**D**) Z-score plot of three replicates of fly repurposing screen test compounds (red circles) versus negative (cyan circles) control wells.

**Figure 3**. Chemical structures of cross-validated drug repurposing hits. (**A**) theaflavin monogallate. (**B**) pomiferin. (**C**) quercetin. (**D**) 3,4-didesmethyl-5-deshydroxy-3'-ethoxyscleroin. (**E**) aripiprazole. (**F**) phenylbutazone. (**G**) benserazide.

**Figure 4**. 20,240-compound novel lead discovery screens of *png-1* homozygous mutant worms and *Pngl* heterozygous mutant flies. (**A**) Worm screen Z-score plot of 20,240 test compounds in

triplicate. Replicate 1 is shown as red circles. Replicate 2 is shown as red triangles. Replicate 3 is shown as red squares. The mean negative control Z-score is indicated by the red line. The mean positive control Z-score is indicated by the cyan line (**B**) Fly screen Z-score plot of 20,240 test compounds in triplicate. Replicate 1 is the left panel. Replicate 2 is the center panel. Replicate 3 is the right panel.

**Figure 5**. Aripiprazole worm and fly cross-validation data. (**A**) $Pngl^{-/-}$ homozygote larvae treated with 10μM, 50μM and 100μM aripiprazole compared to untreated controls. (**B**) $png-1$ homozygote larvae treated with 25μM aripiprazole in the presence of 205nM Bortezomib (Bzb) or 27.5μM carfilzomib (Czb).

**Supplemental Material**. Summary of cross-validation experiments for worm and fly hit compounds.

**Supplemental Figure 1**. Carfilzomib dose-response curve of $png-1$ homozygous worms.

**Supplemental Figure 2**. Z-score plot of 31 hits from the $Pngl^{+/-}$ fly repurposing screen.

**Supplemental Figure 3**. Box plots showing size separation of positive control versus negative control wells in the 20,240-compound lead discovery screen of $png-1$ homozygous worms.

**Supplemental Figure 4**. Box plots showing size separation of positive control versus negative control wells in the 20,240-compound lead discovery screen of $Pngl^{+/-}$ fly larvae.

## References

**Costa M.D.C., Ashraf N.S., Fischer S., Yang Y., Schapka E., Joshi G., McQuade T.J., Dharia R.M., Dulchavsky M., Ouyang M., Cook D., Sun D., Larsen M.J., Gestwicki J.E., Todi S.V., Ivanova M.I., Paulson H.L.** (2016). Unbiased screen identifies aripiprazole as a modulator of abundance of the polyglutamine disease protein, ataxin-3. *Brain*. **139**: 2891-2908.

**Dziekan J.M., Yu H., Chen D., Dai L., Wirjanata G., Larsson A., Prabhu N., Sobota R.M., Bozdech Z., Nordlund P.** (2019). Identifying purine nucleoside phosphorylase as the target of quinine using cellular thermal shift assay. *Sci. Transl. Med.* **11**: eaau3174.

**Enns G.M., Shashi V., Bainbridge M., Gambello M.J., Zahir F.R., Bast T., Crimian R., Schoch K., Platt J., Cox R., Bernstein J.A., Scavina M., Walter R.S., Bibb A., Jones M., Hegde M., Graham B.H., Need A.C., Oviedo A., Schaaf C.P., Boyle S., Butte A.J., Chen R., Chen R., Clark M.J., Haraksingh R., FORGE Canada Consortium, Cowan T.M., He P., Langlois S., Zoghbi H.Y., Snyder M., Gibbs R.A., Freeze H.H., Goldstein D.B.** (2014). Mutations in NGLY1 cause an inherited disorder of the endoplasmic reticulum-associated degradation pathway. *Genet. Med.* **16**, 751-758.

**Fenteany G., Standaert R.F., Lane W.S., Choi S., Corey E.J., Schreiber S.L.** (1995). Inhibition of proteasome activities and subunit-specific amino-terminal threonine modification by lactacystin. *Science*. **268**, 726-731.

**Galeone A., Han S.Y., Huang C., Hosomi A., Suzuki T., Jafar-Nejad H.** (2017). Tissue-specific regulation of BMP signaling by Drosophila N-glycanase 1. *eLife*. **6**: e27612.

**Glynn S.J., Gaffney K.J., Sainz M.A., Louie S.G., Petasis N.A.** (2015). Molecular characterization of the boron adducts of the proteasome inhibitor bortezomib with epigallocatechin-3-gallate and related polyphenols. *Org. Biomol. Chem.* **13**: 3887-3899.

**Golden E.B., Lam P.Y., Kardosh A., Gaffney K.J., Cadenas E., Louie S.G., Petasis N.A., Chen T.C., Schonthal, A.H.** (2009). Green tea polyphenols block the anticancer effects of bortezomib and other boronic acid-based proteasome inhibitors. *Blood.* **113**: 5927-5937.

**Grimberg K.B., Beskow A., Lundin D., Davis M.M., Young P.** (2011). Basic leucine zipper protein Cnc-C is a substrate and transcriptional regulator of the Drosophila 26S proteasome. *Mol. Cell Biol.* **31**: 897-909.

**Kikuchi T., Tottori K., Uwahodo Y., Hirose T., Miwa T., Oshiro Y., Morita S.** (1995) 7-(4-[4-(2,3-Dichlorophenyl)-1-piperazinyl]butyloxy)-3,4-dihydro-2(1H)-quinolinone (OPC-14597), a new putative antipsychotic drug with both presynaptic dopamine autoreceptor agonistic activity and postsynaptic D2 receptor antagonistic activity. *J Pharmacol. Exp. Ther.* **274**: 329-336.

**Kong J., Peng M., Ostrovsky J., Kwon Y.J., Oretsky O., McCormick E.M., He M., Argon Y., Falk M.J.** (2018). Mitochondrial function requires NGLY1. *Mitochondrion*. **38**, 6-16.

**Lam C., Ferreira C., Krasnewich D., Toro C., Latham L., Zein W.M., Lehky T., Brewer C., Baker E.H., Thurm A., Farmer C.A., Rosenzweig S.D., Lyons J.J., Schreiber J.M., Gropman A., Lingala S., Ghany M.G., Solomon B., Macnamara E., Davids M., Stratakis C.A., Kimonis V., Gahl W.A., Wolfe L.** (2017). Prospective phenotyping of NGLY1-CDDG, the first congenital disorder of deglycosylation. *Genet. Med.* **19**, 160-168.

**Lehrbach N. and Ruvkun G.** (2016). Proteasome dysfunction triggers activation of SKN-1A/Nfr1 by the aspartic protease DDI-1. *eLife*. **5**:e17721.

**Martin M., Hiroyasu A., Guzman R.M., Roberts S.A., Goodman A.G.** (2018). Analysis of Drosophila STING Reveals an Evolutionarily Conserved Antimicrobial Function. *Cell Rep.* **23**: 3537-3550.

**Osuna-Lugue J., Rodriguez-Ramos A., Gamez-Del-Estal M.D.M., Ruiz-Rubio M.** (2018). Behavioral Mechanisms That Depend on Dopamine and Serotonin in *Caenorhabditis elegans* Interact With the Antipsychotics Risperidone and Aripiprazole. *J Exp. Neurosci.* **12**: 1179069518798628.

**Owings K.G., Lowry J.B., Bi Y., Might M., Chow C.Y.** (2018). Transcriptome and functional analysis in a Drosophila model of NGLY1 deficiency provides insight into therapeutic approaches. *Hum. Mol Genet.* **27**: 1055-1066.

**Paek J., Lo J.Y., Narasimhan S.D., Nguyen T.N., Glover-Cutter K., Robida-Stubbs S., Suzuki T., Yamamoto M., Blackwell T.K., Curran S.P.** (2012). Mitochondrial SKN1-Nrf mediates a conserved starvation response. *Cell Metab.* **16**: 526-537.

**Palikaras K., Lionaki E., Tavernarakis N.** (2015). Coordination of mitophagy and mitochondrial biogenesis during ageing in C. elegans. *Nature*. **521**: 525-528.

**Radhakrishnan S.K., den Besten W., Deshaies R.J.** (2014). p97-dependent retrotranslocation and proteolytic processing govern formation of active Nrf1 upon proteasome inhibition. *eLife*. **3**: e01856.

**Rodriguez T.P., Mast J.D., Hart T., Lee T., Sand P., Perlstein E.O.** (2018). Defects in the neuroendocrine axis contribute to global development delay in a Drosophila model of NGLY1 Deficiency. *G3*. **8**: 2193-2204.

**Shapiro D.A., Renock S., Arrington E., Chiodo L.A., Liu L., Sibley D.R., Roth B.L., Mailman R.** (2003). Aripiprazole, a novel atypical antipychotic drug with a unique and robust pharmacology. *Neuropsychopharmacology.* **28**: 1400-1411.

**Smirnova N.A., Haskew-Layton R.E., Basso M., Hushpulian D.M., Payappilly J.B., Speer R.E., Ahn Y.H., Rakhman I., Cole P.A., Pinto J.T., Ratan R.R., Gazaryan I.G.** (2011). Development of Neh2-luciferase reporter and its application for high throughput screening and real-time monitoring of Nrf2 activators. *Chem. Biol.* **18**: 752-765.

**Suzuki T., Huang C., Fujihira H.** (2016). The cytoplasmic peptide:N-glycanase (NGLY1) – Structure, expression and cellular functions. *Gene*. **577**, 1-7.

**Tomlin F.M., Gerling-Driessen U.M., Liu Y.C., Flynn R.A., Vangala J.R., Lentz C.S., Clauder-Muenster S., Jakob P., Mueller W.F., Ordoñez-Rueda D., Paulsen M., Matsui N.,**

19

**Foley D., Rafalko A., Suzuki T., Bogyo M., Steinmetz L.M., Radhakrishnan S.K., Bertozzi C.R.** (2017). Inhibition of NGLY1 inactivates the transcription factor Nrf1 and potentiates proteasome inhibitor cytotoxicity. *ACS Cent. Sci.* **3**, 1143-1155.
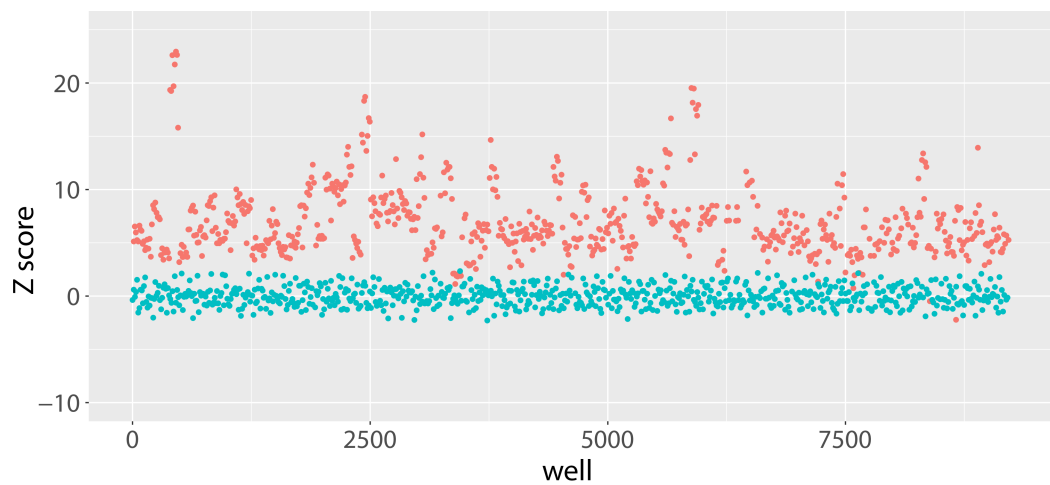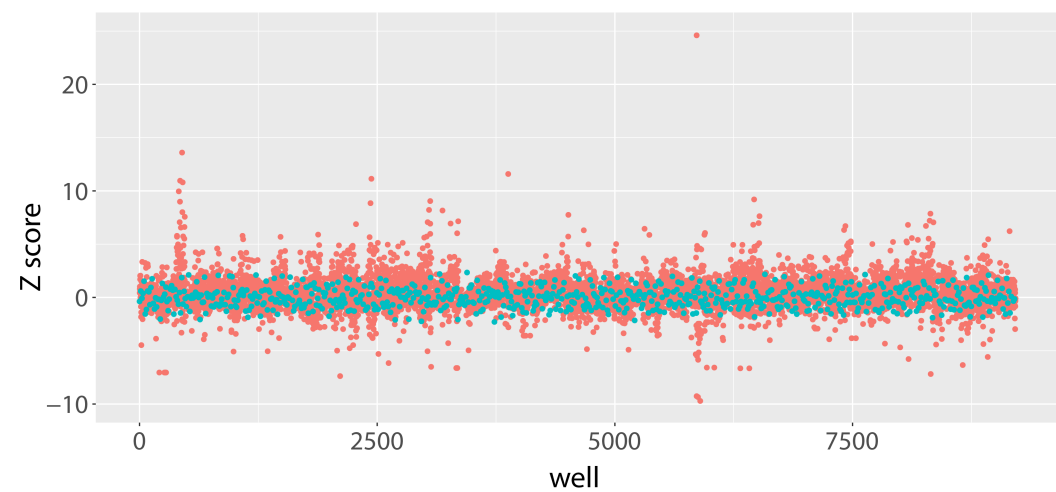
**Tsakiri E.N., Sykiotis G.P., Papassideri I.S., Terpos E., Dimopoulos M.A., Gorgoulis V.G., Bohmann D., Trougakos I.P.** (2013). Proteasome dysfunction in Drosophila signals to an Nrf2-dependent regulatory circuit aiming to restore proteostasis and prevent premature aging. *Aging Cell.* **12**: 802-813.

**van Keulen B.J., Rotteveel J., Finken M.J.J.** (2019). Unexplained death in patients with NGLY1 mutations may be explained by adrenal insufficiency. *Physiol. Rep.* **7**: e13979.
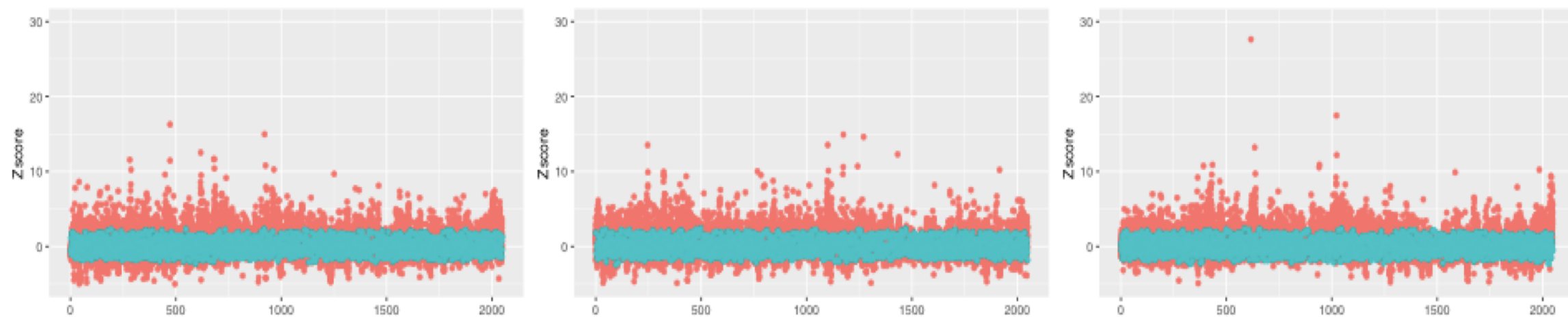
**Wu X., Wu F.H., Wang X., Wang L., Siedow J.N., Zhang W., Pei Z.M.** (2014). Molecular evolutionary and structural analysis of the cytosolic DNA sensor cGAS and STING. *Nucleic Acids Res.* **42**: 8243-8257.

**Yang K., Huang R., Fujihira H., Suzuki T., Yan N.** (2018). N-glycanase NGLY1 regulates mitochondrial homeostasis and inflammation through NRF1. *J Exp. Med.* **215**, 2600-2616.
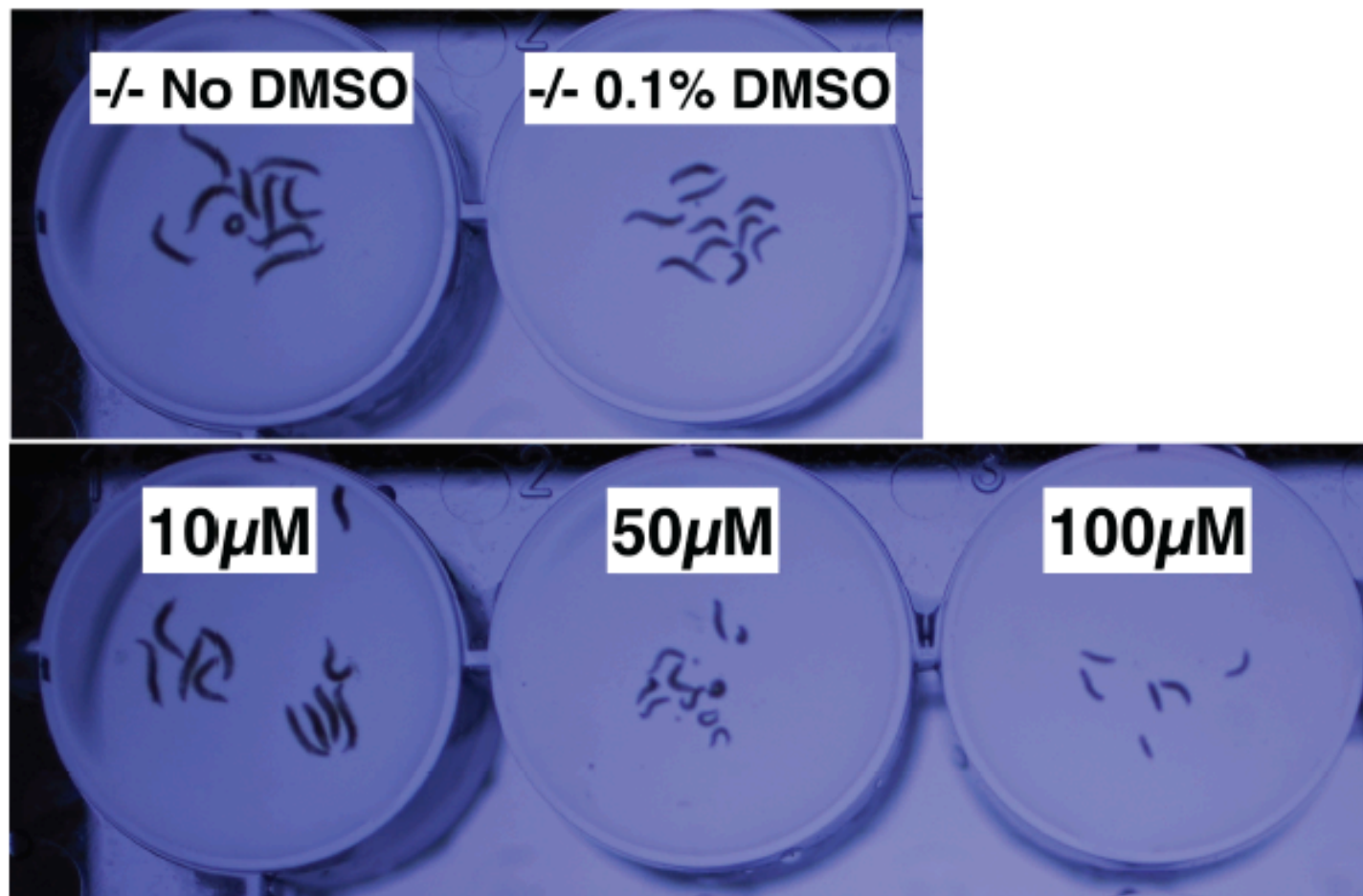
**A**



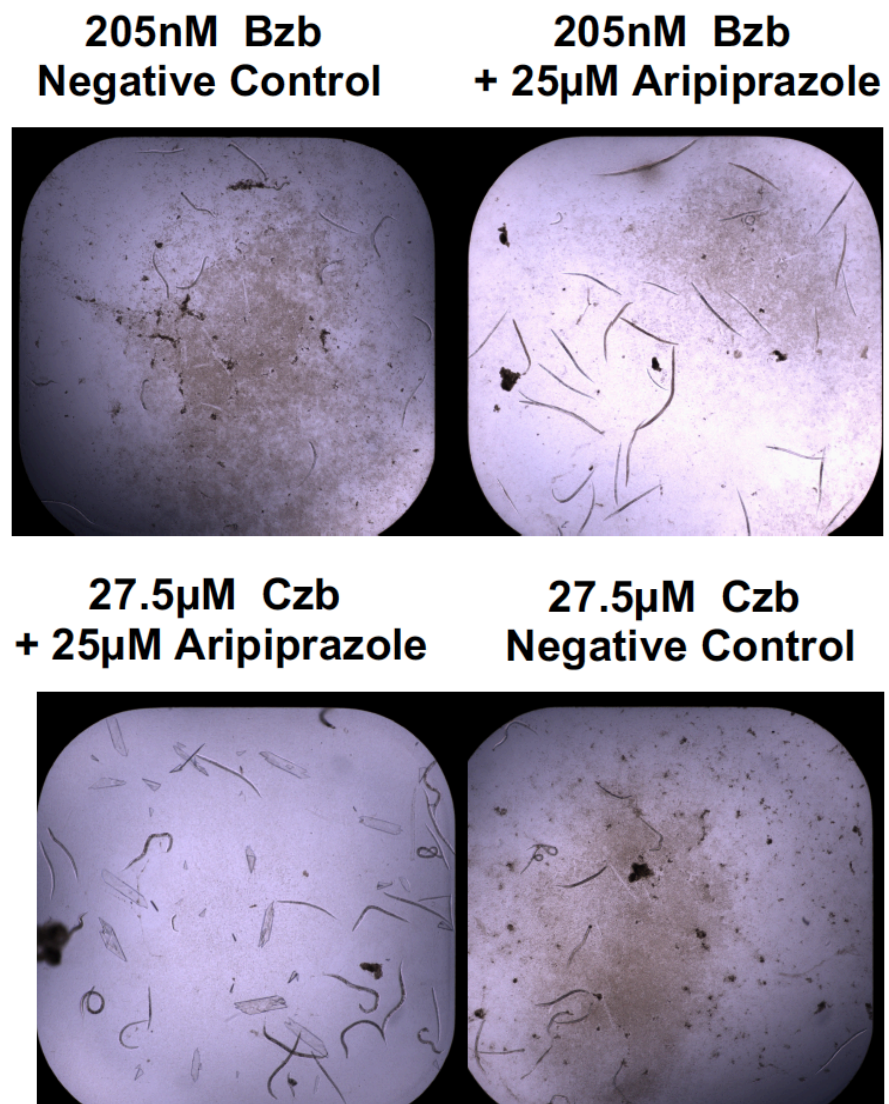| | No bortezomib | 26nM bortezomib | 0.1$\mu$M bortezomib | 1.64$\mu$M bortezomib | 6.5$\mu$M bortezomib | 13$\mu$M bortezomib |

**B**

**A**

| | |
|---|---|
| A01 | C23 |
| K12 | K13 |
| C18 | N14 |
| Replicate 1 | |

| | |
|---|---|
| A01 | C23 |
| K12 | K13 |
| C18 | N14 |
| Replicate 2 | |

| | |
|---|---|
| A01 | C23 |
| K12 | K13 |
| C18 | N14 |
| Replicate 3 | |

**B**

Rep 1

Rep 3

Rep 2

89 suppr.
85 enh.

100 suppr.
74 enh.

63 suppr.
51 enh.

107 suppr,
109 enh.

**C**

Z score

well

**D**

Z score

well

**A**

**B**

**C**

**D**

**E**

**F**

**G**

Worm NGLY1 Chembridge 20K - Hit Compounds

**A**

-/- No DMSO | -/- 0.1% DMSO

10μM | 50μM | 100μM

**B**

205nM Bzb
Negative Control

205nM Bzb
+ 25μM Aripiprazole

27.5μM Czb
+ 25μM Aripiprazole

27.5μM Czb
Negative Control

NGLY Carfilzomib Curve

Worm NGLY1 Chembridge 20K
Batch 1, PL0001-PL0020